COMPLEMENTARY DIAGNOSTICS FOR MONITORING SOOT FORMATION IN MODEL FLAMES BY PIMS AND LII AND APPLICATION OF SOOT DIAGNOSTICS TO TECHNICAL COMBUSTION

Klaus Peter Geigle, Jochen Zerbs, Horst-Henning Grotheer, Kai Hoffmann, Joachim Happold

Institute of Combustion Technology, German Aerospace Center (DLR), Stuttgart, Germany

Introduction

Soot particulates are known to be a health hazard upon emission close to the earth surface and are considered as influencing the global climate when released into certain layers of the atmosphere. The first effect is due to their transportation deep into the respiratory system when being small enough, potentially carrying hazardous molecular species, the second one due to acting as condensation kernels influencing cloud formation and, consequently, the earth's radiative balance. To understand soot formation a precise determination of in-flame soot properties is desirable. On the other hand, their characterization at the exhaust of combustion devices is required for determining potential health hazards. No single diagnostic technique is capable of providing all important soot parameters under all potential ambient conditions. Therefore, understanding and application of complementary diagnostics are necessary to provide the required data. An important factor in employing different techniques is to understand the correlation between typically different parameter definitions. SMPS, for example, measures mobility diameters, while photo-ionization mass spectrometry (PIMS) determines masses, and laser-induced incandescence (LII) measures primary particle diameters.

The following sections start with an inter-comparison of different diagnostics for particle size measurements in model flames. PIMS is employed to identify different types of soot precursor species, first in premixed laminar flames and then in a technical application, i.e. the exhaust tract of a modern Diesel car engine. Finally a short overview is given on application of imaging LII for soot concentration maps in an aero-engine combustor at realistic pressure, following the ICAO definition.

Comparing different diagnostics for in-flame soot measurements

The investigated premixed ethylene/air flames were stabilized on a stainless steel water-cooled, porous plug burner (McKenna) with a fixed total gas flow of 10 sl/min a range of equivalence ratios ϕ. To prevent flame flickering, the flame was stabilized by a cylindrical steel plate with a thickness of 20 mm and a diameter of 60 mm, fixed at a height above the burner (HAB) of 21 mm. Besides the equivalence ratio scan in the standard measurement location of 12 mm above the burner, measurements were made at various HAB along the burner axis for ϕ=2.1 [1]. While SMPS is a widely used commercial tool this section shall focus on time-resolved LII (TiRe LII) and photo ionization mass spectrometry. Those diagnostics are complementary as PIMS can measure from molecular species up to small primary soot particles with a high mass resolution that even allows for structural guesses. LII, on the other hand, is not dependent on sampling from the flame, thus not changing flame properties nor suffering problems with sample line blockages when sampling high soot concentrations. It can measure primary particle sizes from a few nm up to several tens of nm. In contrast to PIMS, the capability for size distributions is limited.

The LII setup is relatively straight forward, passing a 0.4 x 8 mm^2 large 1064 nm laser sheet through the flame and detecting the excited LII emission in a right angle with photomultiplier tubes equipped with suitable filters at 400 and 700 nm. Data analysis followed the approach described by [2], allowing for computation of the main energy transfer mechanisms involved in LII (laser light absorption, surface sublimation, conduction and radiation).

The PIMS apparatus has been recently described [3]. Sample gas concentrations and residence times are decreased from flame ambience conditions through a pressure drop across the sampling nozzle and this leads to a reduction of subsequent reactions (Fig. 1). The sample gas flow is drawn through the pulsed sampling valve (modified Parker valve) via a U-

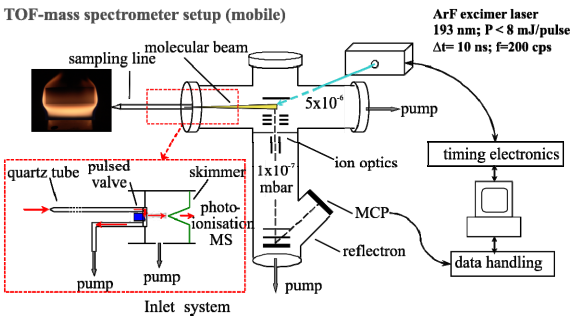

Fig. 1: Illustration of the PIMS setup suitable for flame or exhaust gas sampling. Main components are the inlet system, the time of flight mass spectrometer and the ionization laser.

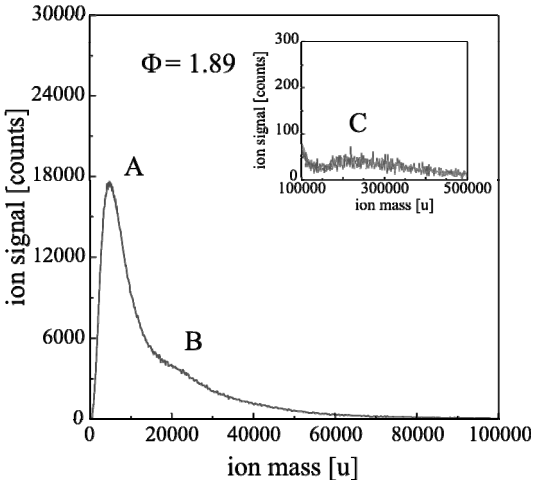

Fig. 2: Flame measurements by PIMS for a premixed flame slighty above the sooting threshold. Different signatures are visible.

shaped tubing which discharges sample gas into the valve body through a lateral bore.This design avoids any stagnation of the reactive sample gas. Downstream of the valve is a skimmer and an additional pumping stage so that the working pressure in the ion source of the MS can be kept around 10^{-6} to 10^{-5} mbar. Ionization is provided by pulsed moderate laser energies in the UV. The setup is suitable for both in-flame measurements and exhaust gas sampling. A representative size distribution determined by PIMS for a sample taken from a moderately sooting flame is shown in Fig. 2. With this moderate mass resolution mass ranges even beyond 1.000.000 u are accessible. This allows the detection of small primary particles (C). In the precursor mass range two distinct features (A and B) can be differentiated.

Comparison of the diagnostics [1] shows a generally good agreement in overlap regions. While LII is not capable to determine bimodal distributions it can easily measure inside moderate to high concentrations where probe sampling fails. In the precursor regime PIMS is the only reliable diagnostic tool. The intermediate range is covered by all diag

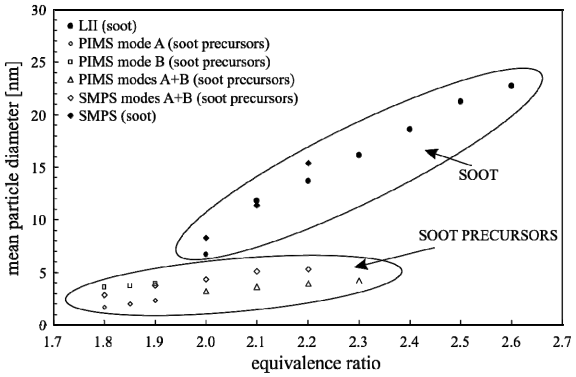

Fig. 3: Mean particle diameters determined by different diagnostics in differently rich premixed flames.

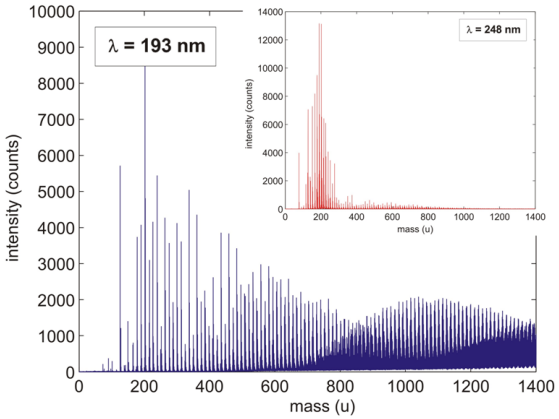

Fig. 4: Mass spectra of an ethylene/oxygen flame with ionization laser wavelengths of 193 nm and 248 nm (inset).

nostics. As SMPS monitors mobility diameter and TiRe LII primary particle size, agreement of both indicates that aggregation of primary particles is weak under these conditions.

PIMS for soot precursor characterization

Recent high resolution transmission electron microscopy (TEM) measurements confirm that a primary soot particle shows up as an inner core surrounded by an outer shell [4]. Only the outer shell is rigidly composed by graphitic structures whereas the inner core contains fine particles surrounded by carbon networks and is relatively unstable.

In our lab, we measured highly resolved mass spectra with a stationary setup moderately different from that shown in Fig. 1 for different low pressure premixed flames, mainly varying fuel, equivalence ratio and dilution [5]. A key feature of the technique was the use of an ArF excimer laser (193 nm) for ionization, in comparison to frequently used longer wavelengths, for example provided by a KrF excimer laser emitting at 248 nm. Using 193 nm excitation we were able to extend the range of detectable ions far beyond conventionally reported mass ranges that are indicative for stable PAHs. Studying potential structures based on the received mass spectra indicates that the hilly structure visible

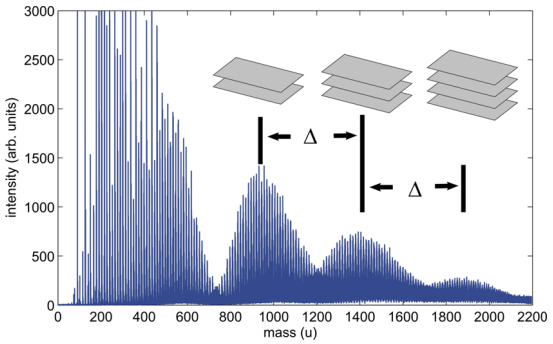

Fig. 5: Spectrum of an acetylene/oxygen flame (193 nm ionization laser wavelength, C/O = 1.3).

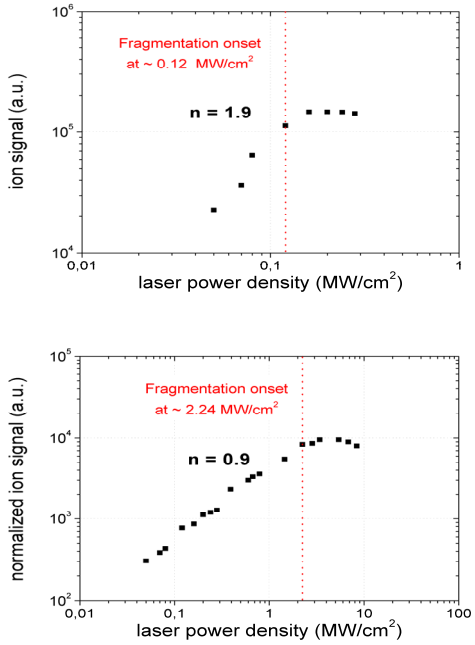

Fig.6: Particle signals as a function of the laser fluence for two types of nanoparticles (top cluster- or PAH-type particles, bottom stack-type particles.

in Figs. 4 and 5 probably originates from stacked aromatic compounds each layer having a mass of about 450 u. Depending on the flame conditions, especially flame temperature, either simple PAHs (below 500 u) or stacks (n·450 u) were formed favourably. Both types of species show different characteristics. As mentioned above, one criteria is the wavelength of the ionizing photons. Stacks can not be excited with lower photon energy than 200 nm. When using 193 nm for ionization and varying the employed laser fluence, the simple PAHs show a ionization order of 2 while stacks can be ionized with a single photon. Given that the stacked PAHs behave similar to solid state matter (such as in the case of carbon graphite) one can assume, that the reason why they cannot be detected with 248 nm laser wavelength lies in the fast internal energy dissipation which is typical for solid state matter. The mutual interaction leads to a reduced work function and thus enables single photon ionization (IO = 1) with 193 nm wavelength. In contrast, simple (=single layer) PAHs can not be ionized by a single photon. Another effect detectable upon variation of the laser fluence is the significant difference in the onset of fragmentation. PAHs are less stable than stacks indicated by a fragmentation threshold 10 fold lower than that of stacks. Beyond this laser fluence the detected ion signal no longer increases but rather stays constant or even decreases (fig. 6). Another difference is the C/H ratio of the different species (see [5] for more details) and the oxidation behaviour towards oxygen.

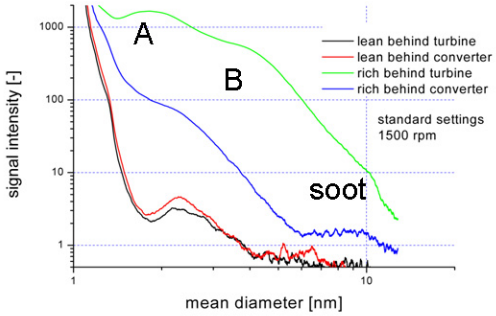

Fig. 7: Mass spectra detected for different operating conditions before and after the catalytic converter.

PIMS measurements in the exhaust system

Recently, the mobile setup shown in fig. 1 was used for measurements immediately after the compressor and after the catalytic converter of a modern, 2.4 l Diesel engine; a first application of this type of diagnostics to our knowledge. The experiments were successful, identifying the same two distinct soot precursor modes described above (fig. 7) in a realistic exhaust system. Between rich and lean operation of the engine the intensities varied by a factor of 1000. However, even at lean operating conditions, precursor species were present in the exhaust gases behind the turbine. At the given very low lean soot concentrations, thermo-gravimetric analyses described this type of soot as more reactive.

Comparing the results measured before and after the catalytic converter it appears that the catalyst influences the larger mode more significantly. The smaller mode emitted at lean conditions remains stable and seems to pass the catalyst. Note that we have not yet accounted for different residence time in the reactive flow when comparing measurements before and after the catalyst. Consequently it is not yet clear whether the described effect originates in surface reactions or is rather being caused by a self-reaction in the gas phase. It has to be born in mind that coagulation rate coefficients for very small particles are under debate. The ionization behaviour of both detected modes differs, similar to the results described above for the fundamental flame. Again, mode A has an ionization order of 2 and a relatively low fragmentation threshold while the larger mode B can be ionized with one single photon.

Besides the similarities found between exhaust gases emitted from a modern engine and our fundamental flame, a more detailed analysis of the described recent measurements is ongoing.

2D LII as a tool supporting engine development

Modern aero-engine technologies have improved rapidly making use of the fact that technical combustion processes can be made accessible by laser optical diagnostics. Applying laser-based methods to realistic combustors offers the opportunity to di

Nomenclature	p [bar]	T(air,in) [K]	ϕ (global)	ϕ (pilot)
Idle, 7% ICAO	4	470	0.2	0.2
Approach, 30% ICAO	9.5	590	0.264	0.12
Cruise-Var1	16.5	590	0.36	0.065
Cruise-Var2	16.5	670	0.36	0.065
Cruise	16.5	670	0.36	0.036
85% ICAO	20	725	0.4	0.054

Table 1: Operating conditions of the studied technical combustor; ϕ(pilot) is contained in ϕ(global), i.e. for *idle*, main injection is not employed.

rectly visualise combustion parameters and use the experimental data for validation purposes provided the boundary conditions are well defined. Both approaches promote the understanding of soot chemistry under technical conditions. On the other hand, technical combustion conditions represent a real challenge to the application of laser diagnostics. Laser-induced incandescence (LII) in particular is a technique that offers many advantages and unique capabilities for the characterisation of soot distributions in combustion [6]. The following section deals with the application of 2D LII as a monitoring tool for soot concentration mapping, making use of the proportionality of LII intensity and local soot concentrations. Measurements have been performed up to 23 bars. Soot distributions for standardised ICAO (International Civil Aviation Organization) conditions *idle*, *approach*, *cruise* and "*85% ICAO*" and similar operating conditions (table 1) are presented.

For the described experiments performed at the ONERA Palaiseau M1 test facility, a maximum pressure of 23 bars with 1.6 kg/s air at 725 K preheat temperature were applied. The fuel lines to provide staging (pilot and main) through the fuel nozzle were separately controlled. The spray flame fed by the fuel nozzle is stabilised inside a combustion

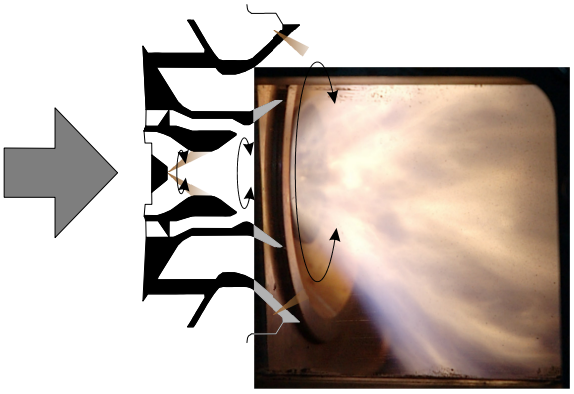

Fig. 8: Schematic of the fuel injector, including pilot (on the axis) and main (annular) and a picture at moderately rich conditions. Flow is from the left to the right.

chamber having a 105 mm x 105 mm squared cross section and a length of 82 mm before converging to the combustor exit. Large quartz windows are used for good optical access. Their maintenance is provided by a strong film cooling: 26% of the total combustor air flushes the windows' inner surface.

In the studied technical fuel nozzle, typical for modern aero-engine injectors, kerosene can be injected either axially (pilot) through an air blast nozzle or radially through circumferential fuel holes (main). While the two inner swirled air flows serve to atomise the pilot fuel (see Fig. 8) the main fuel is multi-point-injected directly into the outer swirled air flow. For a visual impression a picture at moderately sooting conditions is implemented into the schematic.

The 10 Hz laser output at 1064 nm used for LII excitation was transformed into a thin laser sheet and operated slightly beyond the LII plateau regime where signal is only dependent on soot concentration and not on laser fluence [6]. Perpendicular to the excitation in a plane through the burner axis, a ICCD (PCO, Dicam Pro) recorded soot luminosity and LII at 450 nm with 60 ns gates each. The camera's double frame option allows determination of the flame background 500 ns before the laser pulse, i.e. at exactly the same flame conditions. In spite of being weak in intensity, the first frame contains valuable information about the line-of-sight soot distribution of the flame. Due to the combustor window dimensions, not all of the flame is imaged onto the ICCD cameras. Images were quantified by a separate calibration using an atmospheric flame of known soot content.

In Fig. 9 soot distributions are shown for the studied ICAO standard conditions: *cruise, idle*, *approach* and "*85% ICAO"*. The degree of asymmetry in the soot distribution varies with condition and in particular the *cruise* condition shows the highest asymmetry. This asymmetry is not primarily caused by laser absorption. Rather it follows an inhomogeneous air inflow probably caused by the fuel supply pipe in the plenum. It is similarly visible in pure flame emission images without employing a laser. Note that atmospheric calibration for LII probably is not completely valid at increased pressure as the signal decay becomes faster due to stronger conduction cooling of the LII heated particles. This might

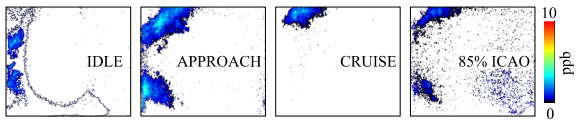

Fig. 9: Spatially resolved, time-averaged soot distributions for defined ICAO conditions.

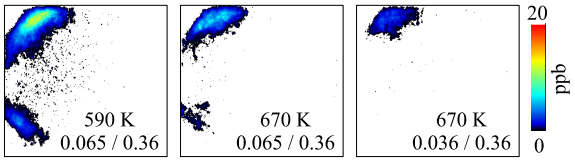

Fig. 10: Influence of air inlet temperature on soot formation (left to centre, Var1 and Var2) and fuel distribution at constant global ϕ (centre to right); right is cruise. Note the different colour bar relative to Fig. 9.

result in higher soot concentrations for the respective operating conditions than indicated in the colour bar. Assuming a worst case factor of 6 for the 20 bar test case the resulting soot concentrations are still significantly low, even compared to a household candle of approx. 1-2 ppm. Peak concentrations in single shot images are higher by a factor up to 30. This can be explained by the typically very small soot signatures, mostly covering only 1-5% of the image area, and their highly dynamic behaviour. For the *idle* representation it must be noticed that strong combustor window pollution occurred during the measurements. The introduced contour line represents the limit of soot luminosity dropping to zero. The sequence additionally shows the decrease of pilot fuel contribution that is injected close to the combustor axis and some mm upstream the burner front plate. Accordingly, the soot cloud forms closest to the burner exit and axis under *cruise* conditions and is increasingly shifted downstream and to larger radial distance from the burner axis.

Fig. 10 shows the trend of soot formation at different air inlet temperature for constant fuel injection (left and centre image). In principle soot formation should be kinetically controlled and thus augment with increased temperature. This behaviour is found for prevaporised kerosene combustion [7]. In contrast, the effect is counter-balanced in kerosene spray flames since increased temperature accelerates vaporisation of the spray followed by improved mixture and reduction of locally rich compositions. Shifting the fuel injection from pilot towards main at constant global equivalence ratio (Fig. 10, centre to right, right is *cruise*) reduces soot production while soot formation occurs more lifted from the nozzle. Distribution of the fuel through multi-holes rather than through the central pilot optimises the mixture under these operating conditions, thus reducing local fuel-rich spots and soot formation.

For a deeper understanding of soot formation under the given technical conditions, soot data shall be compared to OH and kerosene LIF maps determined under equal operating conditions [8]. However, formed soot concentrations remain low at all studied conditions while the peak location depends on fuel staging. LII proved well suitable to monitor soot concentrations under the given highly technical conditions.

To conclude, this manuscript shows the usefulness of employing complementary techniques for soot diagnostics. Moreover it provides some insight into rarely employed PIMS and the type of information that can be received. Finally both diagnostics, PIMS and LII proved applicability to technical questions.

References

[1] R. Stirn, T. Gonzalez Baquet, S.R. Kanjarkar, W. Meier, K.P. Geigle, H.H. Grotheer, C. Wahl, M. Aigner, Combust. Sci. Technol. 181, 329-349 (2009).

[2] H.A. Michelsen, J. Chem. Phys. 118, 7012 (2003).

[3] H.H. Grotheer, K. Hoffmann, K. Wolf, S. Kanjarkar, C. Wahl, M. Aigner, Combust. Flame 156, 791 (2009).

[4] X.I. Naydenova, M. Nullmeier, J.Warnatz, P.A. Vlasov, Combust. Sci. Technol. 176, 1667-1703 (2002).

[5] J. Happold, H.H. Grotheer, M. Aigner, Rapid. Commun. Mass Spectrom. 21, 1247-1254 (2007).

[6] R.J. Santoro, C.R. Shaddix, in: K. Kohse-Höinghaus, J.B. Jeffries (Eds.), Applied Combustion Diagnostics. Taylor & Francis, New York, 2002, pp. 252.

[7] U. Meier, C. Hassa, K.P. Geigle, O. Lammel, P. Kutne, Parametric Study of Soot Formation in an Aeroengine Model Combustor at Elevated Pressures by Laser-Induced Incandescence: Effect of the Fuel Phase, Proc. First CEAS European Air and Space Conference, Berlin, Paper 233 (2007).

[8] F. Grisch, M. Orain, E. Jourdanneau, C. Guin, Simultaneous Equivalence Ratio and Flame Structure Measurements in Multipoint Injectors Using PLIF, AIAA-2008-4868, 44th AIAA/ASME/SAE/ASEE Joint Propulsion Conference & Exhibit, 21 - 23 July 2008, Hartford, CT